Journal of Knot Theory and Its Ramifications, Vol. 11, No. 3 (2002) 295–310
© World Scientific Publishing Company

ON MARKOV'S THEOREM

JOAN S. BIRMAN
Department of Mathematics, Barnard College, Columbia University, 2990 Broadway, New York, NY 10027, USA
jb@math.columbia.edu

WILLIAM W. MENASCO
Department of Mathematics, College of Arts and Sciences, University at Buffalo, The State University of New York, Buffalo, NY 14260-2900, USA
menasco@math.buffalo.edu

1 Introduction

Let $\mathcal{X}$ be an oriented link type in the oriented 3-sphere S^3 or $\mathbb{R}^3 = S^3 - \{\infty\}$. A representative $X \in \mathcal{X}$ is said to be a *closed braid* if there is an unknotted curve $\mathbf{A} \subset S^3 - X$ (the *axis*) and a choice of fibration $\mathcal{H}$ of the open solid torus $S^3 - \mathbf{A}$ by meridian discs $\{H_\theta : \theta \in [0, 2\pi]\}$, such that whenever X meets a fiber H_θ the intersection is transverse. The fact that the link X is a closed braid implies that the number of points in $X \cap H_\theta$ is independent of θ, and we call this number the *braid index* of X. The braid index of $\mathcal{X}$ is the minimum value of the braid index of X over all closed braid representatives $X \in \mathcal{X}$.

Closed braid representations of $\mathcal{X}$ are not unique, and Markov's well-known theorem [9] asserts that any two are related by a finite sequence of elementary moves. One of them is *braid isotopy*, by which we mean isotopy in the complement of the braid axis which preserves transversality between X and fibers of $\mathcal{H}$. The other two moves are mutually inverse, and are illustrated in Figure 1. Both take closed braids to closed braids. We call them *stabilization* and *destabilization*, where the former increases the braid index by one and the latter decreases it by one. The 'weight' w denotes w parallel strands, relative to the given projection. The braid inside the box which is labeled P is an arbitrary $(w+1)$-braid.

*The first author acknowledges partial support from the U.S.National Science Foundation, under Grant DMS-9973232.

†The second author acknowledges partial support from the U.S. National Science Foundation under grant DMS-9626884

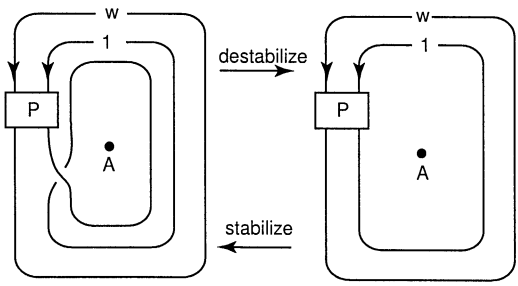

Figure 1: Stabilization and destabilization of closed braids.

Theorem 1 (Markov's Theorem:) *Let X_1, X_2 be closed braid representatives of the same oriented link type $\mathcal{X}$ in oriented 3-space, with the same braid axis* **A**. *Then X_2 may be obtained from X_1 by braid isotopy and a finite number of stabilizations and destabilizations.*

We know of 4 published proofs of Theorem 1, see [3, 8, 10, 11], and each gives a new way of looking at the result. The main result in this paper is to give yet another proof! We hope that our new proof will be of interest because it gives new insight into the geometry, as follows. During recent years a fairly clear picture has emerged of the closed braid representatives of the unknot and unlink. See the main theorem in [6]. Since the operation of taking the braid connected sum of any closed braid representative X of $\mathcal{X}$ with any closed braid representative U of the unknot produces a different closed braid representative of $\mathcal{X}$, a natural question is whether this process of taking braid connected sums with copies of closed braid representatives of $\mathcal{U}$ explains all of the complications in closed braid representatives of $\mathcal{X}$? Our proof of Theorem 1 will clarify this situation. Let X, X' be any two closed braid representatives of the same knot or link type $\mathcal{X}$. We will show that there is an isotopy taking X_1 to an intermediate closed braid X_3 and another isotopy from X_3 to X_2 such that:

1. X_3 is obtained from X_1 by taking the braid connected sum of X_1 with some number of copies of closed braid representatives of $\mathcal{U}$.

2. The isotopy that takes X_3 to X_2 is a push across an embedded annulus $\mathcal{A}_2$ which is a subset of a Seifert surface **F** for X_3. In particular X_2 is a preferred longitude for X_3.

The proof of Theorem 1 is based upon ideas in a forthcoming paper by the authors [7], in which 'Markov's Theorem Without Stabilization' will be

proved. In that paper we will describe a set of moves which suffice to take any closed braid representative of a knot or link to one of minimum braid index for the link type $\mathcal{X}$, with each move preserving or reducing the braid index. The proof which is given here of Theorem 1 will also be used by Nancy Wrinkle in her PhD thesis, which concerns knots which are transverse to the standard contact structure in $\mathbb{R}^3$. It is our hope that the geometry revealed in the new proof of Theorem 1 will have other applications too.

2 Braid foliations

The main result in this paper (Theorem 1) is about the relationship between two closed braid diagrams which represent the same link. However the work which we will do to prove it will not be in the setting of knot diagrams. Rather, we will be dealing with surfaces which our links bound, and with certain *braid foliations* of these surfaces. The foliated surfaces have been used before, in our 6 earlier papers with the common title "Studying links via closed braids", e.g.see [6]. In this section we will review and describe the machinery which we need from these other papers. We will refer the reader to the review article [4] for proofs, whenever possible.

We are given a representative X of an oriented link type $\mathcal{X}$, where X is a closed n-braid with braid axis $\mathbf{A}$. Let $\mathcal{H} = \{H_\theta; 0 \leq \theta \leq 2\pi\}$ be a choice of disc fibers of the braid axis complement, where H_θ denotes a fiber of $\mathcal{H}$. The braid axis and the fibers of $\mathcal{H}$ will be seen to serve the role of a coordinate system in 3-space. We will use it to describe the link (and an auxiliary surface which it bounds) via a set of combinatorial data. The fact that X is a closed braid with respect to $\mathcal{H}$ implies that it intersects each fiber H_θ of $\mathcal{H}$ transversally in exactly n points. The closed braid X is oriented so that it is pointing in the direction of increasing θ at each point of $X \cap H_\theta$.

Our link is assumed to be the boundary of a surface $\mathbf{F}$ of maximum Euler characteristic. After modifying $\mathbf{F}$ we may assume that it admits a special type of singular foliation which was studied and used by the authors in their earlier papers and reviewed in [4]. The foliation is radial in a neighborhood of each point of $\mathbf{A} \cap \mathbf{F}$ (see Figure 2(a)) and transverse to the boundary in a neighborhood of $\partial\mathbf{F}$ (Figure 2(b)). Notice that in Figure 2 the surface $\mathbf{F}$ is naturally oriented by the orientation on X, which is chosen so that the polar angle θ is strictly increasing as we walk along X. This fact orients the associated flow and could be used to orient the foliation, although we have not done so. A *vertex* in the foliation is a point in $\mathbf{A} \cap \mathbf{F}$. The braid axis $\mathbf{A}$ pierces $\mathbf{F}$ from either the negative or the positive side at each pierce point, and we have indicated this by attaching positive or negative signs to the pierce points on $\mathbf{F}$. A *leaf* in the foliation is a component of intersection

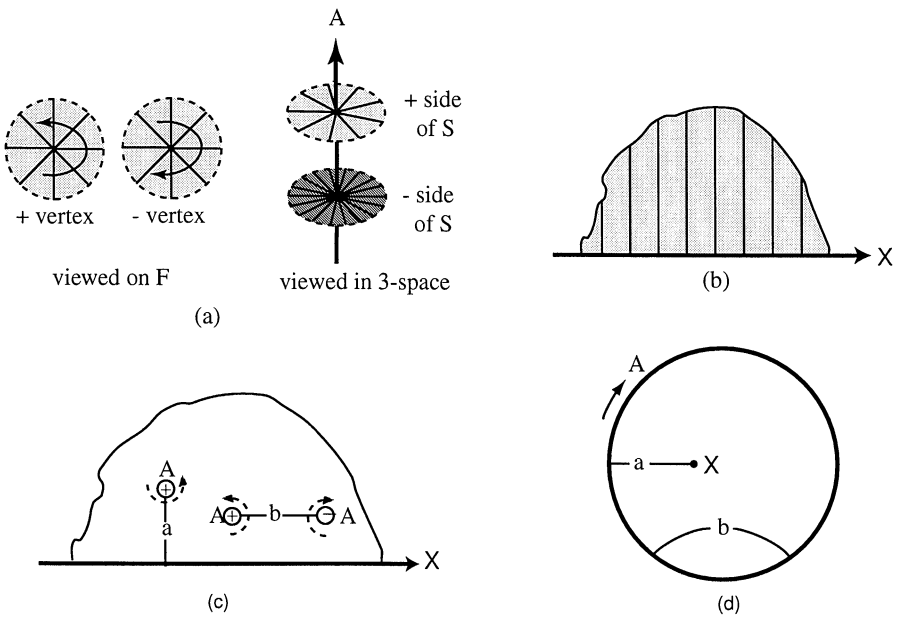

Figure 2: (a)Foliation of $\mathbf{F}$ near a vertex; (b) Foliation of $\mathbf{F}$ near $X = \partial\mathbf{F}$; (c) a-arcs and b-arcs, viewed on $\mathbf{F}$; (d) a-arcs and b-arcs, viewed on a fiber H_θ.

of H_θ with the surface $\mathbf{F}$. We may assume that each leaf is an arc. For details on this assertion and others like it see [4]. Leaves are *singular* if they contain a singularity of the foliation, otherwise they are *non-singular*. The singularities may be assumed to be finite in number and to occur on distinct fibers of $\mathcal{H}$. Every singularity may be assumed to result from a saddle point tangency between $\mathbf{F}$ and a fiber of $\mathcal{H}$. Non-singular leaves are said to be *type a* (respectively *type b*) if they are arcs which have one endpoint on $\mathbf{A} \cap \mathbf{F}$ and the other on $X = \partial\mathbf{F}$ (respectively both endpoints on $\mathbf{A} \cap \mathbf{F}$). See Figure 2(c) and (d). Leaves which have both their endpoints on X do not occur because $\mathbf{F}$ is orientable (see Lemma 1.1 of [4]). When the foliation of $\mathbf{F}$ has all of these properties we call $\mathbf{F}$ a *Markov surface.*

If a vertex is the endpoint of an a-arc, it is always positive (as indicated in Figure 2(a), but it could be either positive or negative at the endpoint of a b-arc. To indicate these differences we will sometimes show a point where the axis pierces $\mathbf{F}$ as as a circle with a $\pm$ sign inside it. Another way to think of the signs on the vertices is that they are *positive* or *negative* according as the outward-drawn oriented normal to $\mathbf{F}$ has the same or opposite orientation as the braid axis at the vertex. This means that when we view the positive side of $\mathbf{F}$, the sense of increasing θ around a vertex will be counterclockwise

(resp. clockwise) when the vertex is positive (resp. negative). The *valence* of a vertex is the number of singular leaves which have endpoints at that vertex.

The foliation may be used to decompose the surface $\mathbf{F}$ into a union of foliated 2-cells, each of which contains exactly one singularity of the foliation. We refer to these 2-cells as *tiles* and the resulting decomposition of $\mathbf{F}$ as a *tiling*. Each tile is a regular neighborhood on $\mathbf{F}$ of its singular leaves. See Figure 3.

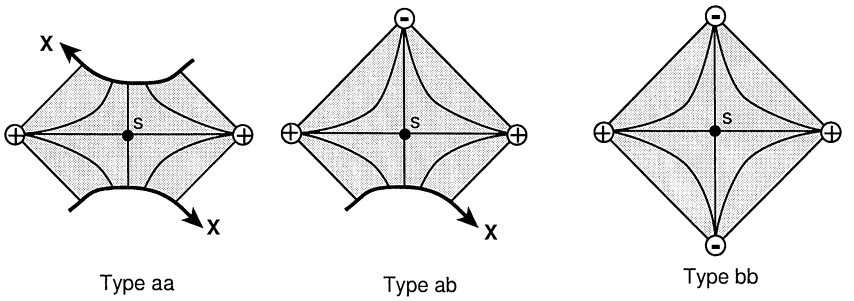

Figure 3: The three tile types.

The *vertices* of the tiles are the points where the braid axis $\mathbf{A}$ intersects the surface $\mathbf{F}$. (There are also other vertices on the graph of singular leaves, but we prefer to exclude them when we refer to tile vertices.) The *edges* of the tiles are non-singular leaves of type a or b. (There are also other tile edges which are subarcs of X, but it will be convenient to ignore those too, just as we ignored the vertices which are on X.)

If two tiles intersect, then they intersect along a non-singular leaf of the foliation, which is then necessarily an edge of type a or b. The tiles fall into three types, according to their foliations. We call them types aa, ab and bb, the notation indicating that in an aa-tile (respectively ab, bb-tile) the leaves which come together before the singularity are both type a (respectively types a and b, both type b). The three tile types are distinguished by the number of their vertices, the types of their non-singular leaves, and the endpoints of their singular leaves. Tiles of type ab and aa meet $X = \partial\mathbf{F}$, but tiles of type bb are contained entirely in the interior of $\mathbf{F}$. Notice also that tiles of type bb, ab, aa each contain 2 positive vertices, but contain $2, 1$ and 0 negative vertices respectively. The segments where X meets a tile of type ab or aa will be seen to 'act like a negative vertex'.

The singularities also have signs. Let s be a singular point of the foliation of a Markov surface $\mathbf{F}$ for a link X, and let H_θ be the disc fiber which contains s. We say that s is *positive* if the outward-drawn oriented normal to the oriented surface $\mathbf{F}$ coincides in direction with the normal to H_θ in the

direction of increasing θ. Otherwise s is *negative.*

A b-arc, when viewed on a fiber of $\mathcal{H}$, divides the fiber into two discs. We say that it is *essential* if both discs are pierced by X. This condition can be seen in the ordering along **A** of the vertices in the tiling of **F**. If the two vertex endpoints of the b-arc have adjacent numbers in the cyclic order on **A**, then the b-arc is inessential, otherwise it is essential. See Figure 4 (a) and (b).

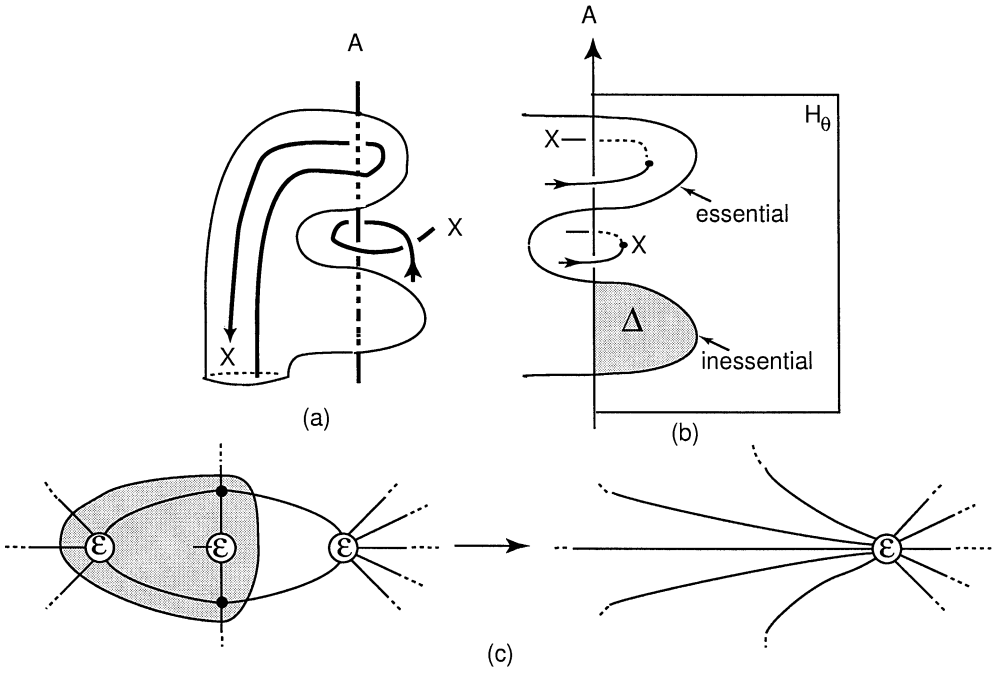

Figure 4: Essential and inessential b-arcs. The bottom two sketches show the changes in typical singular leaves in the foliation when an inessential b-arc is removed.

Lemma 1 *All b-arcs may be assumed to be essential.*

Proof: Any inessential b-arc may be removed by an isotopy of **F**. For details see [4]. The isotopy removes two vertices and two singularities from the foliation. See Figure 4 (c). ||

We next describe two moves which modify the closed braid X and the foliation on **F**, but do not change the link type $\mathcal{X}$. Both change the braid index. Stabilization adds a trivial loop and destabilization removes it. However, there is more to it then that. Our stabilization and destabilization moves are guided by the foliation of the surface. Thus they are moves of the

pair $(X, \mathbf{F})$. As a move on the pair $(X, \mathbf{F})$ our stabilization move is *not* the inverse of our destabilization move, even though they *are* mutually inverse in terms of their effect on X.

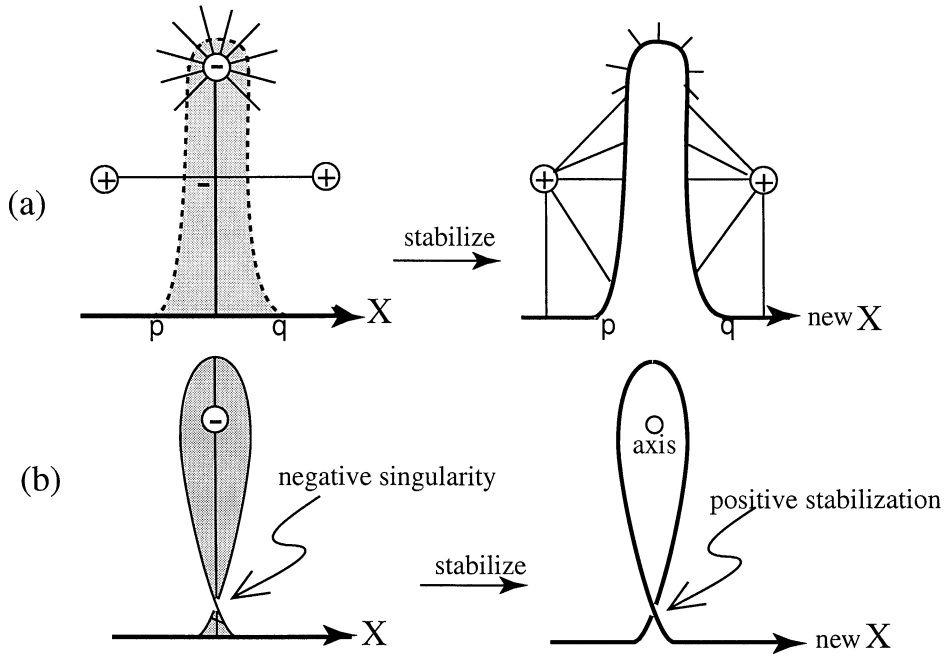

Figure 5: Stabilization along an ab-tile.

Stabilizing along ab tiles: Figure 5 shows a modification in the tiling on $\mathbf{F}$, which we call *stabilizing along an ab tile.* It is realized by pushing X along a disc neighborhood of the singular leaf in an *ab* tile. The boundary of the neighborhood may be chosen to be transverse to the foliation, so the result is a new closed braid representative of the X, bounding a new surface $\mathbf{F}'$ which is tiled, but with one less tile than $\mathbf{F}$. We may visualize the result of the isotopy of X as the addition of a trivial loop, as depicted in Figure 5. This move increases the number of braid strands. As illustrated in Figure 5, its effect on the braid representation of X is to add a "trivial loop" around the axis, increasing the braid index by 1. The effect of our move on the tiling is to eliminate a negative vertex. This will change any *bb* tile that is adjacent to the negative vertex to an *ab* tile.

Destabilizing along end tiles: If the tiling has a vertex of valence 1, then that vertex must be in an *aa*-tile which is glued to itself (see Figure 6), forming a trivial loop. Call such a tile an *end tile.* Removing it, we obtain a

new closed braid, with braid index one less than that of the original one. We call this process destabilizing along an end tile. This move is the inverse of stabilization along an ab tile, as far as its effect on the closed braid, but the two moves are not mutually inverse as regards their effect on the foliation.

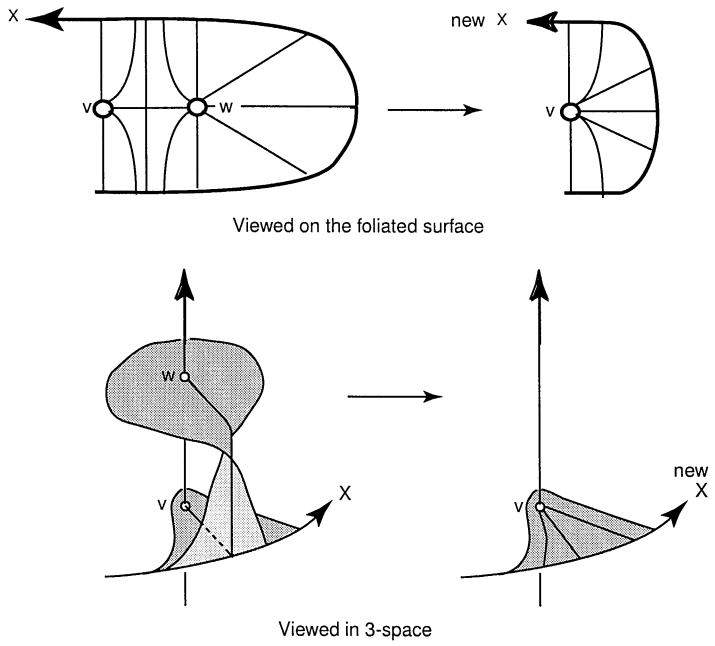

Figure 6: Destabilization along an end tile.

3 A new proof of Markov's Theorem

In our proof the closed braid X will be assumed to be the boundary of a Markov surface $\mathbf{F}$. The central object of study is the pair $(X, \mathbf{F})$ rather than simply the closed braid X. The reader is referred to §2 for the description of the stabilizing and destabilizing moves, as they are reflected in changes in $\mathbf{F}$. They play a central role in our proof.

The new proof of the MT was suggested to us by ideas which were sketched by D. Bennequin in [2], however his proof made use of the characteristic foliation of a surface bounded by a transverse knot, rather than the braid foliations which were described in this paper. We read his proof of the MT many times before we wrote this paper but we only arrived at our present understanding of it comparatively recently, because of its very sketchy nature. (We may, however, have misunderstood what he intended to say.)

If X and X' are closed braids which represent the same link type $\mathcal{X}$, we say that X and X' are *Markov-equivalent* (written $X \equiv X'$) if X can be changed to X' by braid isotopies together with a finite number of stabilizations and destabilizations, i.e. the allowed moves in the MT.

Lemma 2 *Let U be an arbitrary closed braid representative of the unknot and let U_0 be the standard 1-braid representative. Then $U \equiv U_0$.*

Proof: We are given a closed braid representative U of the unknot. It is the boundary of a disc D, and by the methods which are described in §1 we may assume that the disc has a tiling, and that all b-arcs in the tiling are essential. There will in general be p positive vertices and n negative vertices in the tiling. Notice that the braid index is $p - n$, because the braid index is the linking number of U with the braid axis $\mathbf{A}$, but this linking number may also be computed as the algebraic intersection number of $\mathbf{A}$ with a disc D which U bounds, i.e. $p - n$.

If $n > 0$ then there exist ab and/or bb tiles, because there are no negative vertices on an aa tile. However a bb tile can only be adjoined to another bb tile or an ab tile, but since bb tiles do not meet the boundary it is impossible to have only bb tiles. So if $n > 0$, then there exists an ab tile. Let us stabilize along it, as described in §2 and in Figure 5. This eliminates one negative vertex (at the expense of increasing the braid index). The process ends when there are no more negative vertices, i.e. when D is tiled entirely with aa tiles.

Assuming $\mathbf{D}$ is tiled entirely by aa tiles, we consider the graph G which is the union of the non-separating edges in the singular leaves and the vertices in the tiling. The graph G must be a tree, because G is a deformation retract of D and D is a disc. Choose an end-point vertex of this tree and eliminate it by destabilizing, as in Figure 6. This gives a new disc which is again tiled entirely by aa tiles, but with one less tile and so one less singularity. The process ends with a subdisc D, which is foliated radially without singularities. Its boundary is the standard 1-braid representative U_0 of the unknot. ||

Lemma 2 is a very special cases of the MT. Two other special cases follow easily:

Lemma 3 *Let X and U be links which are presented as closed braids. Assume that U represents the unknot. Then X is Markov-equivalent to the braid-connected sum of X and U.*

Proof: The closed braids X and U bound Markov surfaces $\mathbf{F}$ and D, where D is a disc. The surface $\mathbf{F}\#D$ is then a Markov surface whose boundary

is the braid connected sum of X and U. We may simplify the tiling on D by stabilizing along ab-tiles and then deleting valence one vertices, as in the proof of Lemma 2. This produces a Markov equivalence between $X\#U$ and X. ||

Lemma 4 *Let X and X' be closed braids, in general having distinct braid indices. Assume that X' is a preferred longitude for X. Then $X \equiv X'$.*

Proof: Since X' is a preferred longitude for X there is a Seifert surface $\mathbf{F}$ with $\partial\mathbf{F} = X$ and an annulus $\mathcal{A} \subset \mathbf{F}$, with $\partial\mathcal{A} = X - X'$. (Here the minus sign denotes a reversal of the order of X'.) Using the tools which were reviewed in §2 above, we may assume that $\mathbf{F}$ has maximal Euler characteristic and is a Markov surface. Therefore $\mathbf{F}$ admits a tiling. Since X' is a closed braid we may further assume that $X' \subset \mathbf{F}$ is everywhere transverse to the leaves in the foliation. Our plan is to use the tiling on $\mathbf{F}$ and the induced tiling on $\mathcal{A} \cap \mathbf{F}$ to prove that $X \equiv X'$.

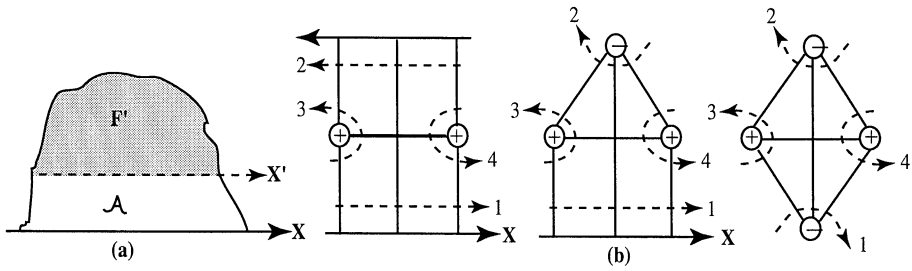

Figure 7: Passages of X' through (a) the annulus bounded by X and X' and (b)tiles of type aa, ab and bb in the annulus.

Recall that $\mathbf{F}$ is a union of tiles of type aa, ab and bb. Let us examine how X' intersects the tiles in the tiling of $\mathbf{F}$. Since $\mathbf{F}$ is tangent to fibers of $\mathcal{H}$ at its singular points, whereas X' (being a closed braid) is everywhere transverse to fibers of $\mathcal{H}$, it follows that X' never passes through a singular point in the tiling, also it is oriented so that it travels clockwise (resp. counterclockwise) whenever it goes around a negative (resp. positive) vertex in the tiling, when we are viewing the positive side of $\mathbf{F}$. Also, whenever subarcs of X' are locally parallel to subarcs of X these subarcs are oriented coherently. It follows that for each of the three tile types there are four different ways that X' can pass through a tile T. These are illustrated in Figure 7(b). We have assigned little numbers $1, 2, 3, 4$ to the four possible components of $X' \cap T$ in each tile T.

The surface $\mathbf{F} = \mathbf{F}' \cup \mathcal{A}$ is oriented, also X' is oriented so that $\mathbf{F}'$ is always on its left and $\mathcal{A}$ on its right, as in Figure 7, whereas X always has

$\mathcal{A}$ on its left. A check of the possibilities then shows that if $X' \cap T$ has more than one component, then the components can only be arcs of type 1 and 2 or type 3 and 4. In the case of tiles of type aa there is an additional constraint which implies that we cannot have components of type 3 and 4 simultaneously. For, if this occurred, then one of the two singular arcs in the tile would begin and end on X and the other would begin and end on X' and both arcs would be in $\mathcal{A}$. However this is impossible because these arcs intersect once in the tile, however $\mathcal{A}$ is an annulus and arcs of the type we have just described must intersect an even number of times. Thus after removing obvious duplications, we are reduced to the 11 cases which are illustrated in Figure 8.

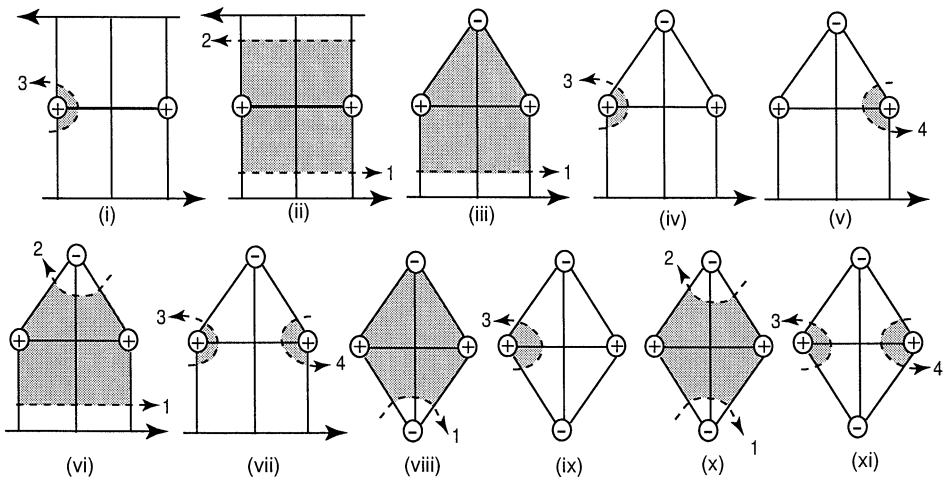

Figure 8: Passages of X' through tiles in the annulus: 11 cases.

One possible measure of the complexity of $\mathcal{A}$ is the number of negative vertices in $\mathcal{A}$. If a tile T has a negative vertex and intersects $X = \partial \mathbf{F}$ then T must be type ab. Let us travel along X, looking for ab tiles. If one occurs then one of its singular leaves begins at X ends at a negative vertex. We may eliminate that negative vertex by stabilizing along the ab tile (see Figure 5). This increases the braid index by 1. The sign of the singularity in the ab tile will determine the sign of the half-twist which we add. This process ends when there are no more singular leaves which have one endpoint on X and the other on a negative vertex. But then, cases (iv),(v),(vii) do not occur. In fact, cases (vi),(viii),(ix),(x) and (xi) also do not occur because each of those presupposes the existence of a negative vertex in $\mathcal{A}$, however if we begin at a negative vertex in $\mathcal{A}$ and travel along singular leaves without leaving $\mathcal{A}$ we must eventually arrive at a singular leaf in $\mathcal{A}$ which has one endpoint at a negative vertex and the other on X, but that is impossible.

The only remaining cases are cases (i),(ii),(iii). If case (i) occurs we may stabilize X' by pushing it across the singular leaf in $\mathcal{A}$. (Equivalently, we could destabilize X by repeatedly deleting vertices of valence 1). This pushes a positive vertex from $\mathcal{A}$ to $\mathbf{F}'$. But then, after some number of such stabilizations, we will have reduced to the situation where only cases (ii) and (iii) occur. That is, there are no singularities whatsoever in $\mathcal{A}$, so the modified braid representatives of X and X' have identical braid structures. The proof of Lemma 4 is complete. ||

Lemma 4 was not the general case of the MT because we assumed that X' is a preferred longitude for X. The next lemma will be needed before we can attack the general case.

Lemma 5 The unlinking lemma [2]. *Let X and X' be links in 3-space $\mathbb{R}^3$ which are not separated by any topological plane $\mathbb{R}^2 \subset \mathbb{R}^3$. Then we may modify the link X' by isotoping it to a link X'' which is separated from X by a plane P in $\mathbb{R}^3$. The isotopy from X' to X'' may be realized by choosing disjoint embedded discs $D_1, \ldots, D_k$ whose interiors are disjoint from X' and X'', with $int(D_i) \cap X$ a point. Each D_i intersects X in an arc $\alpha_i \subset \partial D_i$ and X'' in the closure β_i of the complement of α_i in ∂D_i. The isotopy is a push of $\alpha_1, \ldots, \alpha_k \subset X'$ across $D_1, \ldots, D_k$ to $\beta_1, \ldots, \beta_k \subset X''$.*

Proof: We may assume that $X \cup X'$ is in general position with respect to projection onto a plane which is orthogonal to the braid axis. Think of X as being colored red and X' as being colored green. There are finitely many points where the projected image of green crosses that of red, with each crossing transversal. If, at *every* such crossing, green crosses under red, then X and X' will be unlinked geometrically and there is no obstruction to pushing green below red to separate them. If not, then after a finite number of green-red crossing switches they will be unlinked. Each crossing switch may clearly be described as in the statement of the lemma. ||

Proof of Theorem 1: By hypothesis, we are given closed braids X_1 and X_2 which represent the same oriented link type in 3-space. We must prove that $X_1 \equiv X_2$. We may assume without loss of generality that X_1 and X_2 are situated in distinct half-spaces (so that they are geometrically unlinked), with X_2 far above X_1. To prove that $X_1 \equiv X_2$ we will construct a series of links X_2', X_2'', X_3', X_3, where X_2 is a preferred longitude for X_3 and X_3 is the braid-connected sum of X_1 with some number of copies of the unknot. By Lemma 3 it will follow that $X_1 \equiv X_3$. By Lemma 4 it will follow that $X_3 \equiv X_2$. Therefore we will have proved that $X_1 \equiv X_2$. Figure 9 may be useful to the reader in following the steps of the proof.

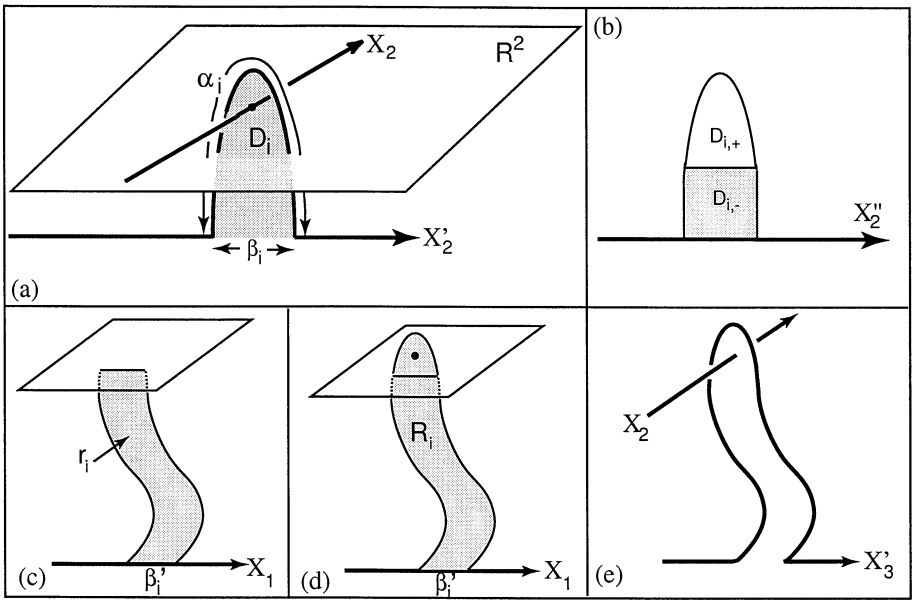

Figure 9: Steps in the construction of X_3

To begin the construction choose a Seifert surface $\mathbf{F}_2$ for X_2 and a preferred longitude $X_2' \subset \mathbf{F}_2$ for X_2. We will assume that X_2' lies in a collar neighborhood of X_2, chosen to be small enough so that X_2' is also a closed braid. We will also assume that X_2' lies below X_2 everywhere except for little hooks where it is forced to travel over a strand of X_2, as in Figure 9(a), because in general $X_2 \cup X_2'$ is not a split link. Applying Lemma 5 we construct a link X_2'' which is isotopic to X_2' and geometrically unlinked from X_2. The isotopy is a push of X_2' across k disjoint discs $D_1, \ldots, D_k$, replacing each $\alpha_i \subset \partial D_i$ by $\beta_i = \partial D_i \setminus \alpha_i$. By modifying the subarcs β_i of X_2'' a little bit, if necessary, we may assume that β_i is transverse to every fiber H_θ of $\mathcal{H}$, so that X_2, X_2' and X_2'' are all closed braids.

It will be convenient to assume that X_2 (resp. X_2'' and X_1) lie in the half-spaces $\mathbb{R}^3_+$ (resp. $\mathbb{R}^3_-$), where the two half-spaces are separated by a plane we refer to as $\mathbb{R}^2$, also that X_2' lies in $\mathbb{R}^3_-$ everywhere except for the k hooks where it passes up and over X_2, intersecting $\mathbb{R}^2$ twice. See Figure 9(a). Passing to Figure 9(b) we think of each disc $D_i, i = 1, \ldots, k$ as a tall thin semi-circular disc which is divided by $\mathbb{R}^2$ into a semi-circular disc $D_{i,+} \subset \mathbb{R}^3_+$ and a rectangular disc $D_{i,-} \subset \mathbb{R}^3_-$, chosen so that $D_{i,-} \cap X_2'' = \beta_i$, where $\beta_i = D_i \cap X_2''$ is the lower edge of the rectangle $D_{i,-}$.

Noting that X_2'' and X_1 both represent $\mathcal{X}$, and that both are in $\mathbb{R}^3_-$, we may find a homeomorphism $g : \mathbb{R}^3_- \to \mathbb{R}^3_-$ which is the identity on $\mathbb{R}^2$ with $g(X_2'') = X_1$. Extend g by the identity on $\mathbb{R}^3_+$ to a homeomorphism

$G : \mathbb{R}^3 \to \mathbb{R}^3$. Let $r_i = G(D_{i,-})$ and let $R_i = G(D_i) = r_i \cup D_{i,+}$. See Figures 9(c) and (d). The facts that (1) G is a homeomorphism which is the identity in $\mathbb{R}^3_+$ and (ii) if $i \neq j$ then $D_{i,-} \cap D_{j,-} = D_i \cap D_j = \emptyset$ tell us that the $r_i's$ and the $R_i's$ are pairwise disjoint embedded discs. By construction $r_i \cap X_2 = \emptyset$, whereas $R_i \cap X_2$ is a single point in the disc $D_{i,+}$. Each r_i joins X_2'' to X_1, meeting X_2'' in the arc β_i and X_1 in the arc $\beta_i' = G(\beta_i)$. Each R_i joins X_2' to X_1, meeting X_2' in α_i and X_1 in β_i.

Let X_3' be the link which is obtained from X_1 by replacing each $\beta_i' \subset X_1$ by $\partial R_i - \beta_i'$. Then X_3' is constructed from X_1 by attaching k pairwise disjoint long thin hooks to X_1. See Figure 9(e). There are two important aspects of our construction:

1. $X_2 \cup X_3'$ has the same link type as $X_2 \cup X_2'$. For, by construction, the homeomorphism $G^{-1} : \mathbb{R}^3 \to \mathbb{R}^3$ sends $X_2 \cup X_3'$ to $X_2 \cup X_2'$.

2. X_3' is the connected sum of X_1 and k copies of the unknot, the i^{th} copy being ∂R_i.

Now recall that by our initial construction we had chosen X_2' to be a preferred longitude for X_2. From (1) it follows that X_3' is also a preferred longitude for X_2. There are 2 cases.

Case 1: If X_3' is isotopic in the complement of the axis to a closed braid, then let X_3 be that closed braid. By construction X_3 is the connected sum of X_1 and k closed-braid copies of the unknot. By Lemma 3 we conclude that $X_1 \equiv X_3$. We already know that X_3 is a preferred longitude for X_2. Changing our point of view, it follows that X_2 is a preferred longitude for X_3. Choose a Seifert surface $\mathbf{F}_3$ for X_3. Holding X_3 fixed, we may then isotope the interior of $\mathbf{F}_3$ so that X_2 lies on $\mathbf{F}_3$. But then X_2 and X_3 cobound a subannulus $\mathcal{A} \subset \mathbf{F}_3$. But then, by Lemma 4, we conclude that $X_3 \equiv X_2$. Therefore $X_1 \equiv X_2$.

Case 2: In general X_3' will not be a closed braid because the two arcs in $\partial r_i - \beta_i \cup \beta_i'$ will in general not be transverse to the fibers of $\mathcal{H}$. In this case we apply Alexander's trick (see [1]) to change the subarcs that are 'in braid position' to a union of arcs which are in braid position. Alexander does this by subdiving any such wrongly ordered arc δ into appropriate smaller arcs, each of which can be pushed across a disc Δ which intersects the axis $\mathbf{A}$ once, as in Figure 10. In this construction Alexander shows that one may always choose the disc Δ so that its interior has empty intersection with X_3'. This is accomplished by choosing the point $\mathbf{A} \cap \Delta$ to have very large or very small z-coordinate. In our situation the fact all of the arcs which are not in braid position are in $\mathbb{R}^3_-$, whereas X_2 is in $\mathbb{R}^3_+$ allows us to assume that all such modifications occur far away from X_2. Therefore $X_2 \cup X_3$ has the same

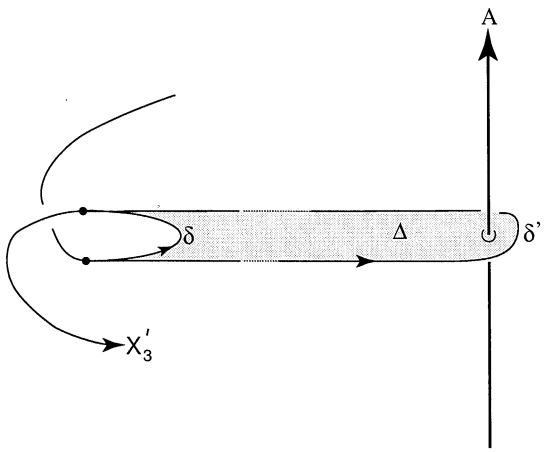

Figure 10: Alexander's trick

link type as $X_2 \cup X_3'$. By the argument for case (1), it then follows that the proof of Theorem 1 is complete. ||

Remark 1: If V and W are closed braid representatives of knots $\mathcal{V}$ and $\mathcal{W}$, and if $X = V\#W$ represents $\mathcal{V}\#\mathcal{W}$, we say that X is the *braid connected sum* of V and W if there is a 2-sphere in 3-space which intersects X twice and intersects the axis twice, separating the closed braids V and W. We stated in §1 that our proof of Theorem 1 would show that X_3 is obtained from X_1 by taking the braid connected sum of X_1 with some number of closed braid representatives of the unknot $\mathcal{U}$, say $U_1, \ldots, U_k$. We have, indeed, shown that there are closed representatives $U_1, \ldots, U_k$ of the unknot and that $X_3 = X_1\#U_1\#\cdots\#U_k$, but braid connected sum seems like a stronger assertion. However, the main result of [5] asserts that in this situation, after a sequence of exchange moves and isotopies in the complement of the braid axis, we may assume that our connected sum of closed braids is in fact the braid connected sum.

Remark 2: In our proof of Theorem 1 we only treated the case of knots, but the proof works equally well for links. A detailed discussion of the case of links (and of many other aspects of the construction given here) will appear in the forthcoming manuscript [7].

References

[1] J. W. Alexander, *A lemma on systems of knotted curves*, Proc.. Nat. Acad. Sci. USA. **9** (1923), 93-95.

[2] D. Bennequin, *Entrelacements et equations de Pfaff*, Asterisque **107-108** (1983), 87-161.

[3] J. S. Birman, *Braids, Links and Mapping Class Groups*, Annals of Math. Studies **82** (1974).

[4] J. S. Birman and E. Finkelstein, *Studying surfaces va closed braids*, J. of Knot Theory and its Ramifications, **7**, No. 3 (1998),267-334.

[5] J. S. Birman & W. W. Menaso, *Studying Links Via Closed Braids IV:Closed Braid Representatives of Split and Composite Links*, *Invent. Math.* **102**, Fasc. 1 (1990), 115-139.

[6] J. S. Birman & W. W. Menaso, *Studying Links Via Closed Braids V: Closed Braid Representatives of the Unlink*, Trans AMS, **329** No. 2 (1992) pp. 585-606.

[7] J. S. Birman & W. W. Menaso, *Stabilization in the braid groups*, manuscript in preparation.

[8] S. Lambropoulou & C. Rourke, *Markov's theorem in 3-manifolds*, Topology and its Applications **78**, Nos. 1-2 (1997), 95-122.

[9] A. A. Markov, *Uber die freie Aquivalenz geschlossener Zopfe*, Recueil Mathematique Moscou, **1** (1935), 73-78.

[10] H. Morton, *Threading knot diagrams*, Math Proc. Camb. Phil. Soc. **99**, 247-260.

[11] P. Traczyk, *A new proof of Markov's braid theorem*, *Knot Theory*, Banach Center Publications **42**, Polish Acad. of Sciences (1998), 409-419.